Search for double-β decay processes in ^{106}Cd with the help of a $^{106}CdWO_4$ crystal scintillator

P. Belli,[1] R. Bernabei,[1,2,*] R. S. Boiko,[3] V. B. Brudanin,[4] F. Cappella,[5,6] V. Caracciolo,[7,8] R. Cerulli,[7] D. M. Chernyak,[3] F. A. Danevich,[3] S. d'Angelo,[1,2] E. N. Galashov,[9] A. Incicchitti,[5,6] V. V. Kobychev,[3] M. Laubenstein,[7] V. M. Mokina,[3] D. V. Poda,[3,7] R. B. Podviyanuk,[3] O. G. Polischuk,[3] V. N. Shlegel,[9] Yu. G. Stenin,[9,†] J. Suhonen,[10] V. I. Tretyak,[3] and Ya. V. Vasiliev[9]

[1]*INFN, Sezione di Roma "Tor Vergata", I-00133 Rome, Italy*
[2]*Dipartimento di Fisica, Università di Roma "Tor Vergata", I-00133 Rome, Italy*
[3]*Institute for Nuclear Research, MSP 03680 Kyiv, Ukraine*
[4]*Joint Institute for Nuclear Research, 141980 Dubna, Russia*
[5]*INFN, Sezione di Roma "La Sapienza", I-00185 Rome, Italy*
[6]*Dipartimento di Fisica, Università di Roma "La Sapienza", I-00185 Rome, Italy*
[7]*INFN, Laboratori Nazionali del Gran Sasso, I-67100 Assergi (AQ), Italy*
[8]*Dipartimento di Fisica, Università dell'Aquila, I-67100 L'Aquila, Italy*
[9]*Nikolaev Institute of Inorganic Chemistry, 630090 Novosibirsk, Russia*
[10]*Department of Physics, University of Jyväskylä, P.O. Box 35 (YFL), FI-40014 Finland*

(Received 11 September 2011; revised manuscript received 9 February 2012; published 13 April 2012)

A search for double β processes in ^{106}Cd was carried out at the Gran Sasso National Laboratories of the INFN (Italy) with the help of a $^{106}CdWO_4$ crystal scintillator (215 g) enriched in ^{106}Cd up to 66%. After 6590 h of data taking, new improved half-life limits on the double β decay processes in ^{106}Cd were established at the level of 10^{19}–10^{21} yr; in particular, $T_{1/2}^{2\nu\varepsilon\beta^+} \geqslant 2.1 \times 10^{20}$ yr, $T_{1/2}^{2\nu 2\beta^+} \geqslant 4.3 \times 10^{20}$ yr, and $T_{1/2}^{0\nu 2\varepsilon} \geqslant 1.0 \times 10^{21}$ yr. The resonant neutrinoless double-electron captures to the 2718-, 2741-, and 2748-keV excited states of ^{106}Pd are restricted to $T_{1/2}^{0\nu 2K} \geqslant 4.3 \times 10^{20}$ yr, $T_{1/2}^{0\nu KL_1} \geqslant 9.5 \times 10^{20}$ yr, and $T_{1/2}^{0\nu KL_3} \geqslant 4.3 \times 10^{20}$ yr, respectively (all limits at 90% confidence level). A possible resonant enhancement of the $0\nu 2\varepsilon$ processes is estimated in the framework of the quasiparticle random phase approximation (QRPA) approach. Radioactive contamination of the $^{106}CdWO_4$ crystal scintillator is reported.

DOI: 10.1103/PhysRevC.85.044610 PACS number(s): 29.40.Mc, 23.40.−s, 27.60.+j

I. INTRODUCTION

Neutrinoless double β decay ($0\nu 2\beta$) is a powerful tool to investigate the properties of the neutrino and of weak interactions. The study of this nuclear decay, forbidden in the framework of the standard model, can allow us to determine the absolute scale of the neutrino mass and its hierarchy, to establish the nature of the neutrino (Majorana or Dirac particle), and to check the lepton number conservation, the possible contribution of right-handed admixtures to the weak interaction, and the existence of Nambu-Goldstone bosons (majorons) [1].

Experimental efforts over the last 70 years have concentrated mainly on the decay modes with emission of two electrons. Allowed in the standard model, the two-neutrino (2ν) $2\beta^-$ decay mode was observed in 10 isotopes with half-lives in the range of 10^{18}–10^{24} yr. For the $0\nu 2\beta^-$ decay mode half-life limits at the level of 10^{23}–10^{25} yr were set for several nuclei (see reviews [2,3] and original studies [4–9]), while positive evidence for ^{76}Ge was published in Ref. [10] and new experiments are in progress to further investigate the latter isotope as well.

The results of the searches for the capture of two electrons from atomic shells (2ε), electron capture with positron emission ($\varepsilon\beta^+$), and emission of two positrons ($2\beta^+$) are at the level of 10^{16}–10^{21} yr (see review [2] and original works [11–27]); although allowed, the two-neutrino mode of these processes has not yet been detected.[1] High-sensitivity experiments to search for neutrinoless 2ε and $\varepsilon\beta^+$ decays are also important because they could clarify a contribution of right-handed admixtures in weak interactions [31].

The isotope ^{106}Cd (the decay scheme is presented in Fig. 1) is among the most widely studied $2\beta^+$ nuclides, thanks to the large energy release ($Q_{2\beta} = 2775.39(10)$ keV [32]) and to the comparatively high natural abundance (1.25 ± 0.06% [33]). It should be stressed that ^{106}Cd is a rather promising isotope also according to the theoretical predictions [31,34–38]. In particular, the calculated half-lives for the two-neutrino mode of the 2ε and $\varepsilon\beta^+$ processes are at the level of $T_{1/2} \sim 10^{20}$–10^{22} yr [35,39–42], reachable with the present low counting technique.

Furthermore, in the case of 0ν capture of two electrons from the K shell (or L and K shells), the energy releases of 2727 keV ($2K$ capture), 2747 keV (KL_1), and 2748 keV (KL_3) are close to the energies of a few excited levels of ^{106}Pd (with $E_{\rm exc} = 2718$, 2741, and 2748 keV). Such a coincidence could give a resonant enhancement of the $0\nu 2\varepsilon$ capture [43–48].

*rita.bernabei@roma2.infn.it
†Deceased.

[1]An indication of $2\beta^+$ decay processes in ^{130}Ba was obtained by the geochemical method [28,29]; however, this result has to be confirmed in a direct counting experiment. It is worth mentioning the work [30] where BaF_2 crystal scintillators were used to search for double β processes in ^{130}Ba.

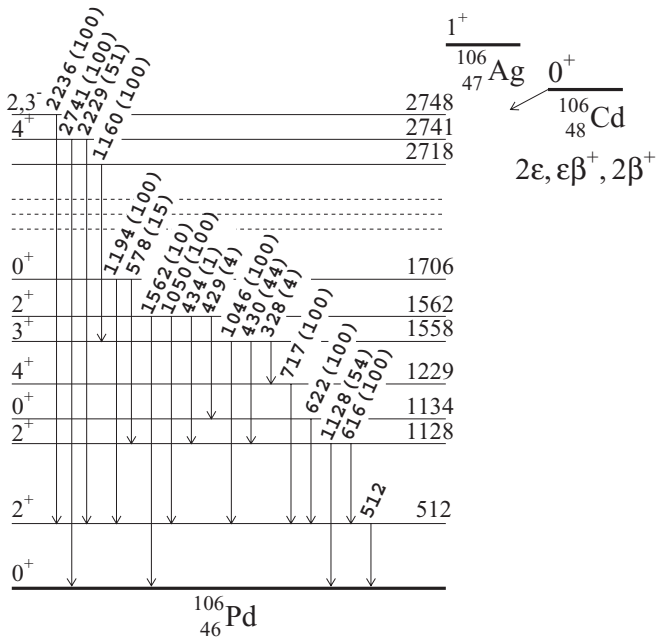

FIG. 1. Simplified decay scheme of ^{106}Cd [52] (levels at 1904–2714 keV are omitted). Energies of the excited levels and of the emitted γ quanta are in keV. Relative intensities of γ quanta are given in parentheses.

Therefore, it is not surprising that the study of ^{106}Cd has a rather long history. The half-life limits at the level of 10^{15} yr could be extracted from old (1952) underground measurements of a Cd sample with photographic emulsions [49], while a search for positrons emitted in $2\beta^+$ decay was performed in 1955 with a Wilson cloud chamber in a magnetic field and with 30 g of cadmium foil; this gave a limit of 10^{16} yr [50]. Measurements of a 153-g Cd sample during 72 h with two NaI(Tl) scintillators working in coincidence were carried out in Ref. [51]; the half-life limits at the level of $\sim 10^{17}$ yr were determined for $2\beta^+$, $\varepsilon\beta^+$, and 2ε processes.

The subsequent studies can be divided into two groups: experiments using samples of cadmium with external detectors for the detection of emitted particles (with enriched ^{106}Cd [22,53] and natural cadmium [39]) and experiments with detectors containing cadmium, namely, semiconductor CdTe and CdZnTe detectors [54,55] and $CdWO_4$ crystal scintillators [7,56,57]. Previous experiments on the search for 2β processes in ^{106}Cd are summarized in Table I.

Data from the experiment, performed at the Solotvina Underground Laboratory (1000 m w.e.), with a 15-cm^3 $^{116}CdWO_4$ crystal scintillator (enriched in ^{116}Cd to 83%, with 0.16% ^{106}Cd), were used to set the limits on the 2β decay of ^{106}Cd at the level of 10^{17}–10^{19} yr [56]. In experiment [39], 331 g of Cd foil was measured at the Frejus Underground Laboratory (4800 m w.e.) with a 120-cm^3 HPGe detector during 1137 h; γ quanta from annihilations of the positrons and from the de-excitation of the daughter ^{106}Pd nucleus were searched for, giving rise to half-life limits at the level of 10^{18}–10^{19} yr. In Ref. [57], a large (1.046-kg) $CdWO_4$ scintillator was measured at the Gran Sasso National Laboratories (3600 m w.e.) over 6701 h. The determined limits on the half-life for the $2\beta^+$ and $\varepsilon\beta^+$ decays were at the level of $\sim 10^{19}$ yr for 0ν and $\sim 10^{17}$ yr for 2ν processes. A small (0.5-g) CdTe crystal was tested as a cryogenic bolometer in 1997 [54]; the achieved sensitivity was $\sim 10^{16}$ yr for $0\nu 2\beta^+$ decay. An experiment [53] was performed in 1999 at the Gran Sasso National Laboratories using an enriched ^{106}Cd (to 68%) cadmium sample (154 g) and two low-background NaI(Tl) scintillators installed in the low-background DAMA/R&D setup during 4321 h; these measurements reached a sensitivity level of more than 10^{20} yr for $2\beta^+$, $\varepsilon\beta^+$, and 2ε processes. A long-term (14 183-h) experiment in the Solotvina Underground Laboratory with enriched $^{116}CdWO_4$ scintillators (total mass of 330 g) was completed in 2003 [7]; in addition, results of dedicated measurements during 433 h with a 454-g nonenriched $CdWO_4$ crystal were also considered [58]. In general, the experimental sensitivity was improved by approximately 1 order of magnitude in comparison with older measurements [56].

There are two running experiments to search for 2β decay of ^{106}Cd: COBRA and TGV-II. $T_{1/2}$ limits in the range of 10^{17}–10^{18} yr were set in the COBRA experiment [55] using CdTe and CdZnTe crystals. In the TGV-II experiment [22,23], 32 planar HPGe detectors are used. Cadmium foils enriched in ^{106}Cd to 75% are inserted between neighboring detectors. The main goal of the TGV experiment is the search for two-neutrino double-electron capture in ^{106}Cd. After 8687 h plus 12 900 h (in two phases of the experiment) of data taking, the limits on double β decay of ^{106}Cd to the ground state and to the excited levels of ^{106}Pd are around 10^{20} yr.

We would like to mention two important advantages of the experiments using detectors containing cadmium: a higher detection efficiency for the different channels of the ^{106}Cd double β decay and the possibility of resolving the two neutrino and the neutrinoless modes of the decay.

Thanks to their good scintillation characteristics, their low level of intrinsic radioactivity, and their pulse-shape discrimination ability (which allows an effective reduction of the background), cadmium tungstate crystal scintillators have been successfully applied in low-background experiments in order to search for double β decay of cadmium and tungsten isotopes [7,16,57], and in order to investigate rare α [59] and β [58,60] decays.

The aim of the present work was to search for 2β processes in ^{106}Cd with the help of a low-background cadmium tungstate crystal scintillator enriched in ^{106}Cd ($^{106}CdWO_4$).

II. EXPERIMENT

The cadmium tungstate crystal (27 mm in diameter and 50 mm in length; mass, 215 g), used in the experiment was developed [61] from deeply purified cadmium [62] enriched in ^{106}Cd to 66%. The scintillator was fixed inside a cavity ($\varnothing 47 \times 59$ mm) in the central part of a polystyrene light-guide, 66 mm in diameter and 312 mm in length. The cavity was filled with high-purity silicon oil. Two high-purity quartz light guides, 66 mm in diameter and 100 mm in length, were optically connected to the opposite sides of the polystyrene light guide. To collect the scintillation light the assembly was viewed by two low-radioactive EMI9265–B53/FL, 3-in.-diameter

TABLE I. Experiments on the search for 2β decay of ^{106}Cd. The range of $T_{1/2}$ limits corresponds to values given for the transitions to the ground state or to the excited levels of ^{106}Pd. More detailed information can be found in the original papers (see also [2]). COBRA and TGV experiments are still running.

Description	$T_{1/2}$ limit (yr)	Year [Ref. No.]
Cd samples between photographic emulsions[a]	$\sim 10^{15}$ ($0\nu 2\beta^+$, $0\nu\varepsilon\beta^+$)	1952 [49]
Cd foil in a Wilson cloud chamber	6×10^{16} ($0\nu 2\beta^+$)	1955 [50]
Cd sample between two NaI(Tl) scintillators in coincidence	$(2.2–2.6) \times 10^{17}$ ($2\beta^+$)	1984 [51]
	$(4.9–5.7) \times 10^{17}$ ($\varepsilon\beta^+$)	
	1.5×10^{17} ($2\nu 2\varepsilon$)	
$^{116}CdWO_4$ crystal scintillator	$(0.5–1.4) \times 10^{18}$ ($0\nu 2\beta^+$)	1995 [56]
	$(0.3–1.1) \times 10^{19}$ ($0\nu\varepsilon\beta^+$)	
	5.8×10^{17} ($2\nu 2\varepsilon$)	
$CdWO_4$ crystal scintillator	2.2×10^{19} ($0\nu 2\beta^+$)	1996 [57]
	9.2×10^{17} ($2\nu 2\beta^+$)	
	5.5×10^{19} ($0\nu\varepsilon\beta^+$)	
	2.6×10^{17} ($2\nu\varepsilon\beta^+$)	
Cd sample measured by HPGe detector	1.0×10^{19} ($2\beta^+$)	1996 [39]
	$(6.6–8.1) \times 10^{18}$ ($\varepsilon\beta^+$)	
	$(3.5–6.2) \times 10^{18}$ (2ε)	
CdTe cryogenic bolometer	1.4×10^{16} ($0\nu\varepsilon\beta^+$)	1997 [54]
^{106}Cd sample between two NaI(Tl) scintillators in coincidence	$(1.6–2.4) \times 10^{20}$ ($2\beta^+$)	1999 [53]
	$(1.1–4.1) \times 10^{20}$ ($\varepsilon\beta^+$)	
	$(3.0–7.3) \times 10^{19}$ (2ε)	
$^{116}CdWO_4$ crystal scintillators	$(0.5–1.4) \times 10^{19}$ ($2\beta^+$)	2003 [7]
	$(0.1–7.0) \times 10^{19}$ ($\varepsilon\beta^+$)	
	$(0.6–8.0) \times 10^{18}$ (2ε)	
CdZnTe semiconductor detectors (COBRA)	$(0.9–2.7) \times 10^{18}$ ($2\beta^+$)	2009 [55]
	$(4.6–4.7) \times 10^{18}$ ($\varepsilon\beta^+$)	
	1.6×10^{17} (2ε)	
^{106}Cd samples between planar HPGe detectors (TGV)	3.6×10^{20} ($2\nu 2\varepsilon$)	2011 [22]
	1.1×10^{20} ($0\nu 2\varepsilon$, 2741 keV)	
	$(1.4–1.7) \times 10^{20}$ ($2\beta^+$)	2011 [23]
	$(1.1–1.6) \times 10^{20}$ ($\varepsilon\beta^+$)	
	1.6×10^{20} ($0\nu 2\varepsilon$, 2718 keV)	

[a]To our knowledge, this was the first underground experiment in history to investigate 2β decay.

photomultiplier tubes (PMTs). The detector was installed deep underground in the low-background DAMA/R&D setup at the Gran Sasso National Laboratories of the INFN (Italy). It was surrounded by copper bricks and sealed in a lowradioactive, airtight copper box continuously flushed with high-purity nitrogen gas to avoid the presence of residual environmental radon. The copper box was surrounded by a passive shield made of high-purity copper, 10 cm of thickness, 15 cm of low-radioactive lead, 1.5 mm of cadmium, and 4 to 10 cm of polyethylene/paraffin to reduce the external background. The shield was contained inside a Plexiglas box, also continuously flushed with high-purity nitrogen gas. An event-by-event data acquisition system recorded the amplitude, the arrival time, and the pulse shape of the events by means of a 1 GS/s 8-bit DC270 Transient Digitizer by Acqiris (adjusted to a sampling frequency of 20 MS/s) over a time window of 100 μs.

The energy resolution of the detector was measured with ^{22}Na, ^{60}Co, ^{133}Ba, ^{137}Cs, ^{228}Th, and ^{241}Am γ sources in the beginning of the experiment. For instance, the energy resolution (full width at half-maximum; FWHM) of the $^{106}CdWO_4$ detector for the γ quanta of ^{137}Cs (662 keV) and of ^{228}Th (2615 keV) was 14.2(3)% and 8.4(2)%, respectively. Two additional calibration measurements were performed: one approximately in the middle and the second one at the end of the experiment with the help of ^{22}Na, ^{60}Co, ^{137}Cs, and ^{228}Th γ sources to test the detector stability. In addition, the energy scale of the detector was checked by using the peaks owing to ^{207}Bi contamination of the $^{106}CdWO_4$ crystal scintillator (see Sec. III D). The energy scale during the experiment was reasonably stable with a deviation in the range of 1%–2%. The data from the calibration measurements were used to estimate the dependence of the energy resolution on the energy. Below 500 keV the energy resolution of the detector to γ quanta with energy E_γ can be described by the function $\mathrm{FWHM}_\gamma = \sqrt{11.2 \times E_\gamma}$, while above 500 keV the data are fitted by $\mathrm{FWHM}_\gamma = \sqrt{-4900 + 21 \times E_\gamma}$, where FWHM_γ and E_γ are given in keV.

The low-background measurements were carried out in three runs, listed in Table II. The energy interval of the data taking was chosen as 0.05–4 MeV in run 1 to investigate the background of the detector at low energy. Taking into account the rather high activity of β active $^{113}Cd^m$ (see the

TABLE II. Low-background measurements with the $^{106}CdWO_4$ crystal scintillator. Times of measurements (t), energy intervals of data taking (ΔE), and background counting rates (BG) in different energy intervals are specified.

Run No.	t(h)	ΔE(MeV)	BG [counts/(yr × keV × kg)] in energy interval		
			0.8–1.0 MeV	2.0–2.9 MeV	3.0–4.0 MeV
1	283	0.05–4.0	474(18)	2.6(6)	0.4(3)
2	2864	0.40–1.8	453(11)	–	–
3	6307	0.57–4.0	412(4)	2.3(1)	0.33(4)

next section), data acquisition was slightly modified in order to avoid the recording of the pulse shapes of all events with an energy lower than 0.4 MeV (run 2); the upper energy threshold was ≈1.8 MeV. In the third run, after some improvement of the data acquisition system, the energy threshold was increased to ≈0.57 MeV and the upper energy threshold was set to 4 MeV (run 3). The data accumulated in run 2 were used to estimate the activity of ^{228}Th in the $^{106}CdWO_4$ crystal by a time-amplitude analysis (see Sec. III A). The first 1320 h of data taking (run 1 + part of run 3) was already analyzed and presented in Ref. [63].

III. DATA ANALYSIS

The energy spectrum accumulated with the $^{106}CdWO_4$ detector in runs 1 and 3 over 6590 h is presented in Fig. 2. The counting rate of ≈24 counts/s below the energy of ≈0.65 MeV is mainly caused by the β decay of $^{113}Cd^m$ with activity of 116(4) Bq/kg. Contamination of enriched ^{106}Cd by β active $^{113}Cd^m$ was found in the low-background TGV experiment [64], where β particles and x rays from thin foils of enriched ^{106}Cd were measured by planar Ge detectors; part of this material was used to produce the $^{106}CdWO_4$ crystal.

Contributions to the background above the energy ≈0.6 MeV were analyzed by means of the time-amplitude and of the pulse-shape discrimination techniques, as well as by the fit of the data with Monte Carlo simulated models of the background.

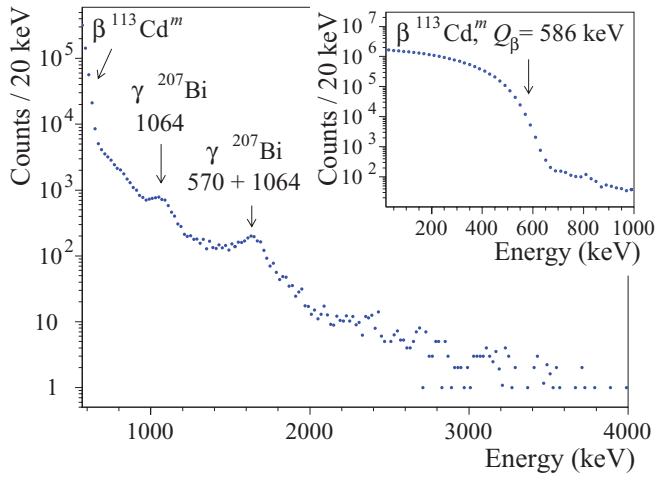

FIG. 2. (Color online) Energy spectrum measured with the $^{106}CdWO_4$ scintillator over 6590 h in the low-background setup. Inset: Decay of β active $^{113}Cd^m$ dominates at an energy of <0.65 MeV (data over 283 h).

A. Time-amplitude analysis of ^{228}Th activity

The arrival time and the energy of each event were used to select the events of the fast decay chain in the ^{232}Th family:[2] ^{224}Ra (Q_α = 5.79 MeV, $T_{1/2}$ = 3.66 d) → ^{220}Rn (Q_α = 6.41 MeV, $T_{1/2}$ = 55.6 s) → ^{216}Po (Q_α = 6.91 MeV, $T_{1/2}$ = 0.145 s) → ^{212}Pb. To select α events from the decays of ^{224}Ra, ^{220}Rn, and ^{216}Po, one should take into account the quenching of the scintillation output in the $CdWO_4$ crystal scintillator, the so-called α/β ratio, defined as the ratio of an α peak position in the γ scale of a detector to the energy of the α particles. The dependence of the α/β ratio on the energy of the α particles measured for the $^{116}CdWO_4$ scintillator [59], $\alpha/\beta = 0.083(9) + 0.0168(13) \times E_\alpha$ (where E_α is in MeV), was used to estimate the positions of ^{224}Ra, ^{220}Rn, and ^{216}Po α peaks in the data accumulated with the $^{106}CdWO_4$ detector. As the first step, all events within the energy interval 0.6–1.8 MeV were used as triggers, while for the second events the time interval 0.026–1.45 s and the same energy window were required. Taking into account the efficiency of the event selection in this time interval (88.2% of ^{216}Po decays), the activity of ^{228}Th in the $^{106}CdWO_4$ crystal was calculated to be 0.042(4) mBq/kg. As the next step, all the selected pairs (^{220}Rn–^{216}Po) were used as triggers in order to find the events of the decay of the mother α active ^{224}Ra. The 1.45- to 111-s time interval (73.2% of ^{220}Rn decays) was chosen to select events in the energy interval 0.6–1.75 MeV. The obtained α peaks from the ^{224}Ra → ^{220}Rn → ^{216}Po → ^{212}Pb chain and the time distributions for the ^{220}Rn → ^{216}Po and ^{216}Po → ^{212}Pb decays are shown in Fig. 3.

The positions of the three α peaks, selected by the time-amplitude analysis in the γ scale of the detector, were used to obtain the following dependence of the α/β ratio on the energy of the α particles, E_α, in the range 5.8–6.9 MeV: $\alpha/\beta = 0.11(2) + 0.011(3) \times E_\alpha$ (where E_α is in MeV). The dependence is in agreement with the data obtained for the $^{116}CdWO_4$ scintillation detector in Ref. [59].

B. Pulse-shape discrimination

As demonstrated in Ref. [68], the difference in pulse shapes in the $CdWO_4$ scintillator can be used to discriminate $\gamma(\beta)$ events from those induced by α particles. The optimal filter method proposed by E. Gatti and F. De Martini in 1962 [69] was applied for this purpose. For each signal $f(t)$,

[2]The technique of the time-amplitude analysis is described in detail, e.g., in Refs. [65,66].

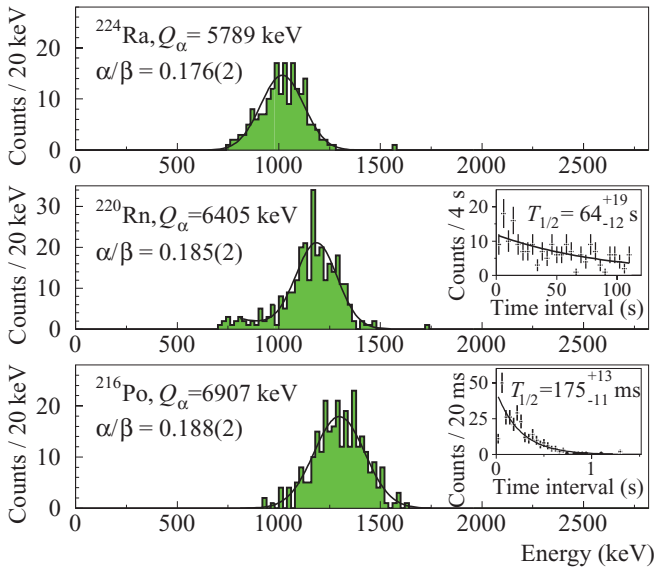

FIG. 3. (Color online) The α peaks of ^{224}Ra, ^{220}Rn, and ^{216}Po selected by the time-amplitude analysis of data accumulated over 9454 h with the $^{106}CdWO_4$ detector. The obtained half-lives of ^{220}Rn (64^{+19}_{-12} s) and ^{216}Po (175^{+13}_{-11} ms) are in agreement with the table values (55.6 s and 145 ms, respectively [67]).

the numerical characteristic of its shape (shape indicator; SI) was defined as $SI = \sum f(t_k) \times P(t_k) / \sum f(t_k)$. Here the sum is over the time channels k, starting from the origin of signal and averaging up to 50 μs, and $f(t_k)$ is the digitized amplitude (at the time t_k) of a given signal. The weight function $P(t)$ was defined as $P(t) = \{f_\alpha(t) - f_\gamma(t)\}/\{f_\alpha(t) + f_\gamma(t)\}$, where $f_\alpha(t)$ and $f_\gamma(t)$ are the reference pulse shapes for α particles and γ quanta measured in Ref. [70]. Using this approach, α events were clearly separated from $\gamma(\beta)$ events as shown in Fig. 4, where the scatterplot of the shape indicator versus energy is depicted for data from the low-background measurements with the $^{106}CdWO_4$ detector. The distribution of the shape indicators for events with energies in the range 0.7–1.4 MeV (shown in the inset in Fig. 4) justifies reasonable pulse-shape discrimination between α particles and γ quanta (β particles), as well as the possibility of rejecting randomly overlapped pulses (mainly caused by β decay of $^{113}Cd^m$).

The energy spectrum of α events selected with the help of pulse-shape discrimination is shown in Fig. 5. As demonstrated in Ref. [59], the energy resolution for α particles is worse than that for γ quanta owing to the dependence of the α/β ratio on the direction of the α particles relative to the $CdWO_4$ crystal axes.[3] As a result, we cannot definitively identify single U/Th α active daughters in the spectrum. Therefore, we set limits only on α activities of U/Th daughters in the $^{106}CdWO_4$ crystal scintillator. For this purpose, the spectrum was fitted in the energy interval 550–1500 keV by a simple model, built of Gaussian functions (to describe the α peaks of U/Th daughters) plus an exponential function to describe the background. The activities of ^{228}Th and ^{226}Ra were restricted taking into account

[3]One could compare the energy resolutions of the α peaks presented in Fig. 3 with the expected resolution for γ quanta (see Sec. II).

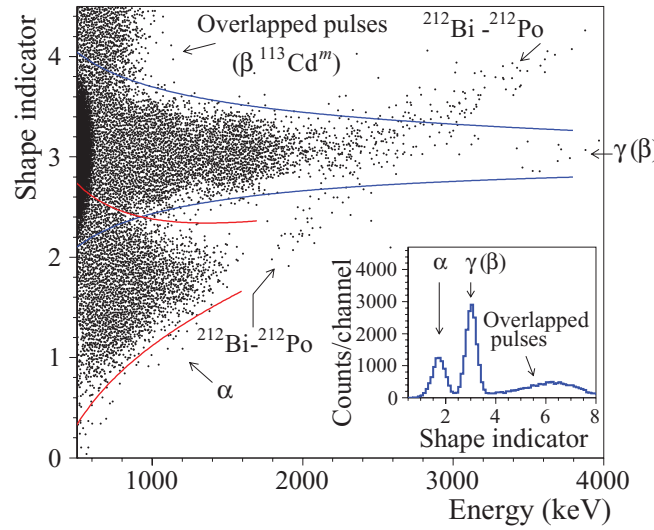

FIG. 4. (Color online) Shape indicators (see text) versus the energy accumulated over 6590 h with the $^{106}CdWO_4$ crystal scintillator in the low-background setup. Three σ intervals for shape indicator values corresponding to γ quanta (β particles) and α particles are depicted. Events with shape indicator values greater than ≈3.8 can be explained by the overlap of events (mainly of β decays of $^{113}Cd^m$ in the crystal), while the population of events in the energy interval ≈1.8–3.8 MeV with shape indicators outside of the $\gamma(\beta)$ region are caused by the decays of the fast ^{212}Bi–^{212}Po subchain of ^{228}Th. Inset: Distribution of the shape indicators demonstrates the efficiency of pulse-shape discrimination among $\gamma(\beta)$, α, and overlapped pulses.

the results of the time-amplitude and of the double pulse (see Sec. III C) analyses. The fit and its components are shown in Fig. 5. The limits on the activity of the U/Th daughters (supposing a broken equilibrium in the chains) are presented in Table III. The total α activity of U/Th in the $^{106}CdWO_4$ crystal is 2.1(2) mBq/kg.

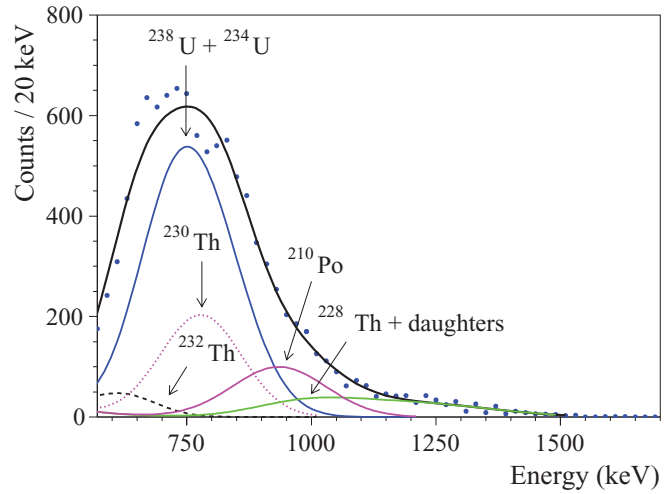

FIG. 5. (Color online) Energy distribution of α events (points) selected by the pulse-shape analysis of data accumulated over 6590 h with the $^{106}CdWO_4$ detector together with the fit (solid line) by a model which includes α decays from the ^{232}Th and ^{238}U families.

TABLE III. Radioactive contamination of the $^{106}CdWO_4$ scintillator determined by different methods (activities are in mBq/kg, while surface contamination by ^{207}Bi is in mBq/cm^2). Data for $^{116}CdWO_4$ and $CdWO_4$ crystal scintillators are presented for comparison.

Chain	Nuclide	Activity		
		$^{106}CdWO_4$	$^{116}CdWO_4$ [7,59,73]	$CdWO_4$ [57,60]
^{232}Th	^{232}Th	$\leqslant 0.07$[a]	$\leqslant$0.08–0.053(9)	$\leqslant 0.026$
	^{228}Th	0.042(4)[b]	0.039(2)–0.062(6)	$\leqslant$(0.003–0.014)
^{238}U	^{238}U	$\leqslant 0.6$[a]	$\leqslant$(0.4–0.6)	$\leqslant 1.3$
	^{230}Th	$\leqslant 0.4$[a]	$\leqslant$(0.05–0.5)	
	^{226}Ra	0.012(3)[c]	$\leqslant 0.005$	$\leqslant$(0.007–0.018)
	^{210}Po	$\leqslant 0.2$[a]	$\leqslant$(0.063–0.6)	$\leqslant 0.063$
Total α activity		2.1(2)[a]	1.4(1)–2.7(3)	0.26(4)
	^{40}K	$\leqslant 1.4$[d]	$\leqslant 0.4$	$\leqslant$(1.7–5)
	^{90}Sr-^{90}Y	$\leqslant 0.3$[d]	$\leqslant 0.2$	$\leqslant 1$
	^{106}Ru	$\leqslant 0.02$[d]	–	–
	$^{110}Ag^m$	$\leqslant 0.06$[d]	0.06(4)	–
	^{113}Cd	182[e]	91(5)	558(4)–580(20)
	$^{113}Cd^m$	116 000(4000)[d]	0.43(6)	$\leqslant$3.4–150(10)
	^{137}Cs	–	2.1(5)	$\leqslant 0.3$
	^{207}Bi internal	$\leqslant 0.7$[d]	0.6(2)	–
	^{207}Bi surface	0.06[d]	–	–

[a]Pulse-shape discrimination (Sec. III B).
[b]Time-amplitude analysis (Sec. III A).
[c]Analysis of double pulses (Sec. III C).
[d]Fit of the background spectrum (Sec. III D).
[e]Calculated taking into account the isotopic abundance of ^{113}Cd in $^{106}CdWO_4$ [61] and the half-life of ^{113}Cd [60].

The pulse-shape analysis also allows us to distinguish the main part of the $^{212}Bi \rightarrow ^{212}Po \rightarrow ^{208}Pb$ events from trace contamination of the crystal by ^{228}Th (see Fig. 4).

C. Identification of Bi-Po events

The search for the fast decays ^{214}Bi ($Q_\beta = 3.27$ MeV, $T_{1/2} = 19.9$ m) $\rightarrow$ ^{214}Po ($Q_\alpha = 7.83$ MeV, $T_{1/2} = 164\mu s$) $\rightarrow$ ^{210}Pb (in equilibrium with ^{226}Ra from the ^{238}U chain) was performed with the help of pulse-shape analysis of the double pulses.[4] Only 11 ^{214}Bi-^{214}Po events were found in the data over 6590 h. Taking into account the detection efficiency in the time window of 1–50 μs (which contains 18.6% of the ^{214}Po decays), one can estimate the activity of ^{226}Ra in the $^{106}CdWO_4$ crystal as 0.012(3) mBq/kg.

To select double pulses produced by the fast chain of the decays ^{212}Bi ($Q_\beta = 2.25$ MeV, $T_{1/2} = 60.55$ m) $\rightarrow ^{212}Po$ ($Q_\alpha = 8.95$ MeV, $T_{1/2} = 0.299$ μs) $\rightarrow$ ^{208}Pb (in equilibrium with ^{228}Th from the ^{232}Th family), a front- edge analysis was developed (see also Ref. [59]). The energy spectrum of the selected ^{212}Bi-^{212}Po events and the time distribution of ^{212}Po decay are presented in Fig. 6. The approach gives the activity of ^{228}Th as 0.051(4) mBq/kg, in reasonable agreement with the result of the time-amplitude analysis.

All the selected Bi-Po events were removed from the $\gamma(\beta)$ spectrum of the $^{106}CdWO_4$ detector.

[4]The technique of the analysis is described, e.g., in Refs. [59,71].

D. Simulation of $\gamma(\beta)$ background, radioactive contamination of the $^{106}CdWO_4$ scintillator

To reproduce the background of the $^{106}CdWO_4$ detector, we consider the contribution of the primordial radioactive isotopes ^{40}K and $^{238}U/^{232}Th$ with their daughters, anthropogenic radionuclides ^{90}Sr-^{90}Y and ^{137}Cs and cosmogenic ^{106}Ru and $^{110}Ag^m$. Anthropogenic ^{90}Sr and ^{137}Cs are the most widespread radionuclides, in particular, after the Chernobyl accident. Contamination of cadmium tungstate by ^{106}Ru and $^{110}Ag^m$ was estimated in Ref. [72], while the presence of $^{110}Ag^m$ in $^{116}CdWO_4$ crystal scintillators was observed in Ref. [73]. Radioactive contamination of the setup (in particular the PMTs and the copper box) can contribute to the background too. The energy distributions of the possible background components were simulated with the help of the EGS4 [74] and GEANT4 [75] codes. The initial kinematics of the particles emitted in the nuclear decays was given by the event generator DECAY0 [76].

The background energy spectrum of the γ and β events, selected by means of the pulse shape, of the front-edge and of the double-pulse analyses, was fitted by a model built from the simulated distributions. The activities of the U/Th daughters were bounded taking into account the results of the time-amplitude and of the pulse-shape analyses. The activities of ^{40}K, ^{232}Th, and ^{238}U in the PMTs were taken from Ref. [77]. The radioactive contaminations of the copper box have been assumed to be equal to those reported in Ref. [78]. In addition, we have added a model of the overlapped $^{113}Cd^m$ β decays, which contribute to the background in the energy region up to $\approx$1 MeV.

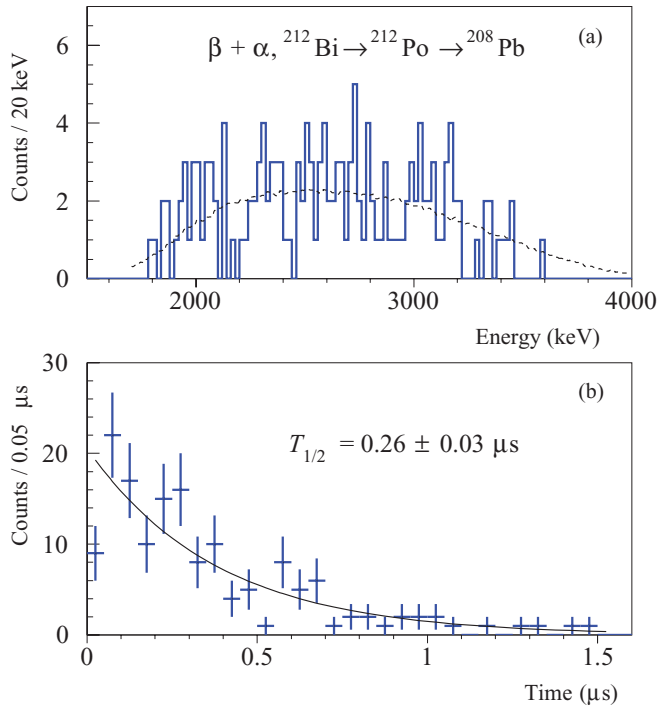

FIG. 6. (Color online) (a) Energy spectrum of ^{212}Bi $\rightarrow$ ^{212}Po $\rightarrow$ ^{208}Pb events in the ^{106}CdWO$_4$ scintillator selected by means of the pulse-shape and of the front-edge analyses (see text) from data accumulated over 6590 h together with the fit (dashed line) of the simulated distribution. (b) Time distribution of ^{212}Po α decay selected by the front-edge analysis. The fit of the time distribution gives a half-life, $T_{1/2} = (0.26 \pm 0.03)$ μs, in agreement with the table value for ^{212}Po (0.299 μs [67]).

Two clear peculiarities in the spectrum of the CdWO$_4$ detector, at (1064 ± 3) and at (1631 ± 5) keV, cannot be explained by the contribution from external γ quanta. Indeed, no similar peaks were observed in the low-background measurements with radiopure ZnWO$_4$ crystal scintillators [79] performed before the present experiment under the same experimental conditions. To explain the peculiarities, we suppose a pollution of the crystal by ^{207}Bi ($T_{1/2} = 31.55$ yr, $Q_{EC} = 2398$ keV [67]). The presence of ^{207}Bi could be caused by contamination of the facilities at the Nikolaev Institute of Inorganic Chemistry (Novosibirsk, Russia) where the ^{106}CdWO$_4$ crystal was grown. A large amount of BGO crystal scintillators is in production in that laboratory. BGO crystal scintillators are typically contaminated by ^{207}Bi at the level of 0.01–10 Bq/kg [80–83]. Moreover, we also cannot exclude the possibility of ^{106}CdWO$_4$ crystal surface contamination at the laboratory of the Institute for Nuclear Research (Kyiv, Ukraine), where the scintillator was diffused and preliminary tested [61] with several γ sources, including an open ^{207}Bi source. Therefore, two distributions of ^{207}Bi (uniformly distributed in the crystal volume and deposited on its surface) were also simulated and added to the background model.

A fit of the spectrum of $\gamma(\beta)$ events in the energy region 0.66—4.0 MeV by the model described above and by the main components of the background are shown in Fig. 7. The fit (χ^2/d.f. $= 111/108 = 1.03$, where d.f. is the number

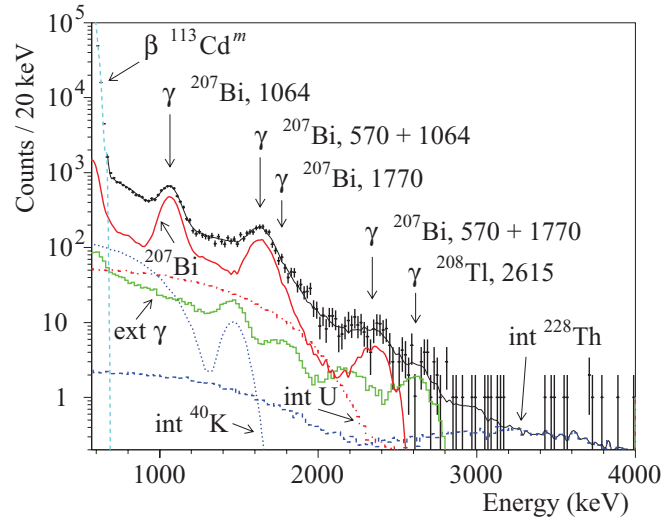

FIG. 7. (Color online) Energy spectrum of $\beta(\gamma)$ events accumulated over 6590 h in the low-background setup with the ^{106}CdWO$_4$ crystal scintillator (points) together with the background model [solid (black) superimposed line]. The main components of the background are shown: the β spectrum of the internal ^{113}Cd^m, the distributions of ^{40}K, ^{228}Th, ^{238}U, and ^{207}Bi (deposited on the crystal surface), and the contribution from external γ quanta from PMTs and the copper box ("ext γ") under these experimental conditions.

of degrees of freedom) confirmed more likely a surface contamination of the crystal scintillator by ^{207}Bi at the level of 3 mBq (0.06 mBq/cm^2). We cannot distinguish the part of the activity owing to bulk contamination and we give a limit only on the internal contamination of the crystal by ^{207}Bi as $\leqslant$0.7 mBq/kg.

There are no other clear peculiarities in the spectrum which could be ascribed to internal trace radioactive contamination. Therefore, we just set limits on the activities of ^{40}K, ^{90}Sr-^{90}Y, cosmogenic ^{106}Ru, and ^{110}Ag^m. A summary of radioactive contamination of the ^{106}CdWO$_4$ crystal scintillator is given in Table III. We hope to clarify further the radioactive contamination of the scintillator in the next stage of the experiment by running the ^{106}CdWO$_4$ crystal scintillator in coincidence/anticoincidence with an ultralow-background HPGe γ detector.

IV. RESULTS AND DISCUSSION

There are no peculiarities in the data accumulated with the ^{106}CdWO$_4$ detector that could be ascribed to the double β decay of ^{106}Cd. Therefore only lower half-life limits can be set by using the formula

$$\lim T_{1/2} = N \times \eta \times t \times \ln 2 / \lim S,$$

where N is the number of ^{106}Cd nuclei in the ^{106}CdWO$_4$ crystal (2.42×10^{23}), η is the detection efficiency, t is the time of measurements, and $\lim S$ is the number of events of the effect searched for, which can be excluded at a given confidence level (CL; all limits on double β processes in ^{106}Cd are given at the 90% CL in the present study).

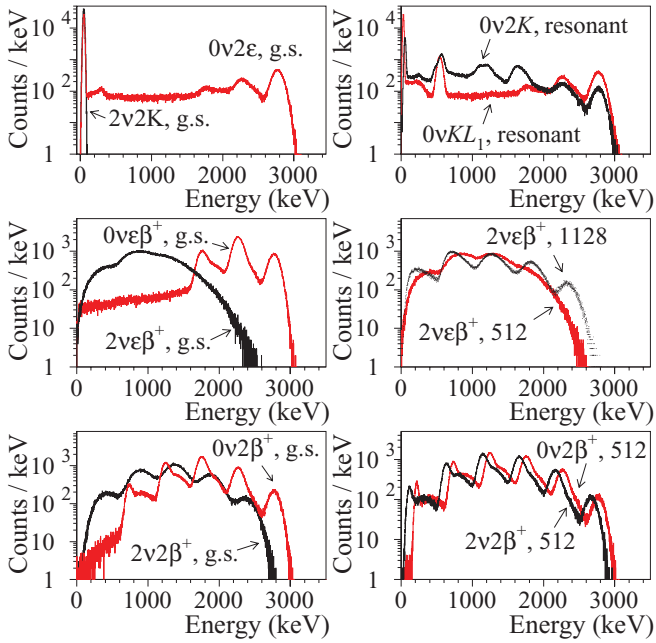

FIG. 8. (Color online) Simulated response functions of the $^{106}CdWO_4$ detector to 2ε, $\varepsilon\beta^+$, and $2\beta^+$ processes in ^{106}Cd.

The response functions of the $^{106}CdWO_4$ detector to the 2β processes in ^{106}Cd were simulated with the help of the EGS4 [74] and the DECAY0 [76] packages (some examples of the simulated spectra are presented in Fig. 8).

A. Double β processes in ^{106}Cd with positron emission

To estimate the value of lim S for the $2\nu\varepsilon\beta^+$ decay of ^{106}Cd to the ground state of ^{106}Pd, the energy spectrum of the γ and β events accumulated over 6590 h with the $^{106}CdWO_4$ detector was fitted by the model built from the components of the background (see Sec. III D) and the effect searched for. The activities of U/Th daughters in the crystals were constrained in the fit taking into account the results of the time-amplitude and pulse-shape analyses. The initial values of the ^{40}K, ^{232}Th, and ^{238}U activities inside the PMTs were taken from Ref. [77], where radioactive contaminations of PMTs of the same model were measured. Radioactive contaminations of the copper were constrained taking into account the data from measurements [84] where copper of a similar quality was used. The best fit (achieved in the energy interval 780–2800 keV with $\chi^2/\text{d.f.} = 93/81 = 1.15$) gives the area of the $2\nu\varepsilon\beta^+$ distribution in the interval of the fit as (26 ± 230) counts, thus providing no evidence for the effect. In accordance with the Feldman-Cousins procedure [85], this corresponds to lim $S = 403$ counts at 90% CL. Taking into account the detection efficiency within the fit window given by the Monte Carlo simulation ($\eta = 0.700$) and the 98% efficiency of the pulse-shape discrimination to select $\gamma(\beta)$ events, we get the following limit on the decay:

$$T_{1/2}^{2\nu\varepsilon\beta^+}(\text{g.s.} \to \text{g.s.}) \geqslant 2.1 \times 10^{20}\text{yr} \ \text{ at } \%\,\text{CL}.$$

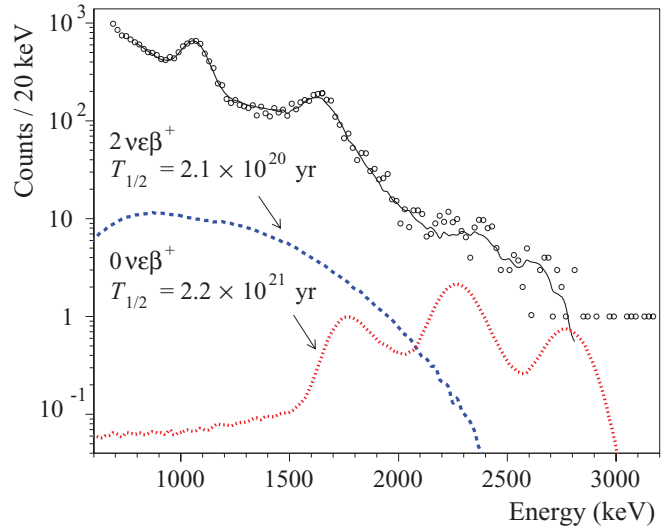

FIG. 9. (Color online) Part of the energy spectrum of γ and β events accumulated with the $^{106}CdWO_4$ detector over 6590 h (circles) and its fit in the energy interval 780–2800 keV (solid line) together with the excluded distributions of $2\nu\varepsilon\beta^+$ and $0\nu\varepsilon\beta^+$ decay of ^{106}Cd.

The excluded energy distribution expected for the two-neutrino $\varepsilon\beta^+$ decay of ^{106}Cd is shown in Fig. 9.

One can prove this result by using the so-called "1σ" approach when the value of lim S can be estimated as the square root of the counts in the energy interval of interest. There are 5462 events in the energy interval 1140–2220 keV, where the detection efficiency for $2\nu\varepsilon\beta^+$ decay is 36%. The method gives a limit $T_{1/2}^{2\nu\varepsilon\beta^+} \geqslant 6.0 \times 10^{20}$ yr at 68% CL, similar to the result acquired by fitting the experimental data with the help of the Monte Carlo simulated models.

The sensitivity to the neutrinoless channel of $\varepsilon\beta^+$ decay is better thanks to the shift of the energy distribution to higher energies. Moreover, there are clear peaks in the spectrum of the $0\nu\varepsilon\beta^+$ process in the energy region 1.6–2.9 MeV, which make the effect much more distinguishable (see Fig. 9). A fit of the data in the energy interval 2000–3000 keV ($\chi^2/\text{d.f.} = 23/25 = 0.92$) gives an area of the effect of (17 ± 13) events (lim $S = 38$ events, $\eta = 0.675$), which corresponds to the following limit on $0\nu\varepsilon\beta^+$ decay of ^{106}Cd to the ground state of ^{106}Pd:

$$T_{1/2}^{0\nu\varepsilon\beta^+}(\text{g.s.} \to \text{g.s.}) \geqslant 2.2 \times 10^{21}\text{yr} \ \text{ at } 90\,\%\,\text{CL}.$$

The 1σ approach gives, for this decay, the limit (there are 187 events in the energy interval 2140–2960 keV, where the detection efficiency for the $0\nu\varepsilon\beta^+$ decay is 62%) $T_{1/2}^{0\nu\varepsilon\beta^+} \geqslant 5.6 \times 10^{21}$ yr at 68% CL, proving the result obtained by fitting the experimental data.

A fit of the data in the energy interval 1200–3000 keV ($\chi^2/\text{d.f.} = 71/65 = 1.09$) gives $S = (92 \pm 52)$ events (lim $S = 177$ events, $\eta = 0.616$) of $2\nu2\beta^+$ decay of ^{106}Cd to the ground level of ^{106}Pd. Therefore, we set the following limit:

$$T_{1/2}^{2\nu2\beta^+}(\text{g.s.} \to \text{g.s.}) \geqslant 4.3 \times 10^{20}\,\text{yr} \ \text{ at } 90\,\%\,\text{CL}.$$

The neutrinoless double-positron decay was restricted by the fit in the energy interval 760–2800 keV ($\chi^2/\text{d.f.} =$

TABLE IV. Half-life limits on 2β processes in ^{106}Cd. Detection efficiencies for the effect searched for (η) and the values of lim S within the energy intervals of fit (ΔE) are presented.

Decay channel	Decay mode	Level of ^{106}Pd (keV)	ΔE (keV)	η	lim S	$T_{1/2}$ limit (yr) at 90% CL	
						Present work	Best previous limits
2ε	2ν	g.s.	–	–	–	–	$\geqslant 3.6 \times 10^{20}$ [22]
		2_1^+ 512	–	–	–	–	$\geqslant 1.2 \times 10^{20}$ [23]
		2_2^+ 1128	660–2780	0.328	99	$\geqslant 4.1 \times 10^{20}$	$\geqslant 5.1 \times 10^{18}$ [39]
		0_1^+ 1134	660–2800	0.367	263	$\geqslant 1.7 \times 10^{20}$	$\geqslant 1.0 \times 10^{20}$ [23]
		2_3^+ 1562	660–2800	0.342	830	$\geqslant 5.1 \times 10^{19}$	–
		0_2^+ 1706	760–2800	0.320	370	$\geqslant 1.1 \times 10^{20}$	–
		0_3^+ 2001	760–2780	0.484	208	$\geqslant 2.9 \times 10^{20}$	–
		0_4^+ 2278	660–3000	0.381	294	$\geqslant 1.6 \times 10^{20}$	–
	0ν	g.s.	1800–3200	0.194	23	$\geqslant 1.0 \times 10^{21}$	$\geqslant 8.0 \times 10^{18}$ [7]
		2_1^+ 512	2040–3200	0.150	36	$\geqslant 5.1 \times 10^{20}$	$\geqslant 3.5 \times 10^{18}$ [39]
		2_2^+ 1128	760–3000	0.465	187	$\geqslant 3.1 \times 10^{20}$	$\geqslant 4.9 \times 10^{19}$ [53]
		0_1^+ 1134	760–3000	0.474	169	$\geqslant 3.5 \times 10^{20}$	$\geqslant 7.3 \times 10^{19}$ [53]
		2_3^+ 1562	760–3000	0.520	186	$\geqslant 3.5 \times 10^{20}$	–
		0_2^+ 1706	760–3000	0.531	262	$\geqslant 2.5 \times 10^{20}$	–
		0_3^+ 2001	1300–3200	0.346	185	$\geqslant 2.3 \times 10^{20}$	–
		0_4^+ 2278	660–3200	0.564	335	$\geqslant 2.1 \times 10^{20}$	–
Res. $2K$	0ν	2718	1280–3000	0.315	91	$\geqslant 4.3 \times 10^{20}$	$\geqslant 1.6 \times 10^{20}$ [23]
Res. KL_1		4^+ 2741	1280–3000	0.238	31	$\geqslant 9.5 \times 10^{20}$	$\geqslant 1.1 \times 10^{20}$ [22]
Res. KL_3		$2, 3^-$ 2748	1300–3000	0.238	69	$\geqslant 4.3 \times 10^{20}$	–
$\varepsilon\beta^+$	2ν	g.s.	780–2800	0.700	403	$\geqslant 2.1 \times 10^{20}$	$\geqslant 4.1 \times 10^{20}$ [53]
		2_1^+ 512	660–3000	0.846	943	$\geqslant 1.1 \times 10^{20}$	$\geqslant 2.6 \times 10^{20}$ [53]
		2_2^+ 1128	1260–3000	0.414	167	$\geqslant 3.1 \times 10^{20}$	$\geqslant 1.4 \times 10^{20}$ [53]
		0_1^+ 1134	1200–3000	0.519	172	$\geqslant 3.7 \times 10^{20}$	$\geqslant 1.6 \times 10^{20}$ [23]
	0ν	g.s.	2000–3000	0.675	38	$\geqslant 2.2 \times 10^{21}$	$\geqslant 3.7 \times 10^{20}$ [53]
		2_1^+ 512	1200–3000	0.936	91	$\geqslant 1.3 \times 10^{21}$	$\geqslant 2.6 \times 10^{20}$ [53]
		2_2^+ 1128	1200–3000	0.678	148	$\geqslant 5.7 \times 10^{20}$	$\geqslant 1.4 \times 10^{20}$ [53]
		0_1^+ 1134	2000–3000	0.240	59	$\geqslant 5.0 \times 10^{20}$	$\geqslant 1.6 \times 10^{20}$ [23]
$2\beta^+$	2ν	g.s.	1200–3000	0.616	177	$\geqslant 4.3 \times 10^{20}$	$\geqslant 2.4 \times 10^{20}$ [53]
		2_1^+ 512	760–2800	0.831	203	$\geqslant 5.1 \times 10^{20}$	$\geqslant 1.7 \times 10^{20}$ [23]
	0ν	g.s.	760–2800	0.956	100	$\geqslant 1.2 \times 10^{21}$	$\geqslant 2.4 \times 10^{20}$ [53]
		2_1^+ 512	780–3000	0.870	92	$\geqslant 1.2 \times 10^{21}$	$\geqslant 1.7 \times 10^{20}$ [23]

$88/82 = 1.07$, $S = -14 \pm 69$, lim $S = 100$, $\eta = 0.956$):

$$T_{1/2}^{0\nu 2\beta^+}(\text{g.s.} \to \text{g.s.}) \geqslant 1.2 \times 10^{21}\ \text{yr at 90 \% CL}.$$

It should be stressed that the mass difference between ^{106}Cd and ^{106}Pd atoms also allows transitions to the excited levels of ^{106}Pd. Thus, we have given limits on the $2\beta^+$ decay of ^{106}Cd to the first excited level of ^{106}Pd (2^+, 512 keV) and on electron capture with positron emission to the few lowest excited levels of ^{106}Pd with spin parity 0^+ and 2^+. The results are presented in Table IV.

B. Double-electron capture in ^{106}Cd

In the case of 2ν double-electron capture in ^{106}Cd from the K or/and L shells, the total energy release in the $^{106}CdWO_4$ detector is in the range from $2E_{L3} = 6.3$ keV to $2E_K = 48.8$ keV (where E_K and E_L are the binding energies of the electrons on the K and L shells of the palladium atom, respectively). Detection of such an energy deposit requires a low enough energy threshold and low background conditions. In our measurements the energy threshold for the acquisition was set too high (because of the background owing to β decay of ^{113}Cd^m) to search for the two-neutrino mode of double-electron capture to the ground state and to the first excited level of ^{106}Pd.

However, we can analyze the existing data to search for 2ν double-electron capture to higher excited levels of ^{106}Pd. For instance, by fitting the background spectrum in the energy interval 660–2780 keV (χ^2/d.f. $= 103/86 = 1.20$, $S = -5 \pm 63$, lim $S = 99$, $\eta = 0.328$) the following half-life limit on $2\nu 2\varepsilon$ decay of ^{106}Cd to the 2_2^+ level (1128 keV) of ^{106}Pd was obtained:

$$T_{1/2}^{2\nu 2\varepsilon}(\text{g.s.} \to 2_2^+) \geqslant 4.1 \times 10^{20}\ \text{yr at 90 \% CL}.$$

The following restriction was set on the $2\nu 2\varepsilon$ decay of ^{106}Cd to the 0_1^+ 1134-keV level of ^{106}Pd by fitting the

experimental spectrum in the energy interval 660–2800 (χ^2/d.f. = 105/87 = 1.21, $S = -5 \pm 163$, lim $S = 263$, $\eta = 0.367$):

$$T_{1/2}^{2\nu 2\varepsilon}(\text{g.s.} \to 0_1^+) \geqslant 1.7 \times 10^{20}\ \text{yr at 90 \% CL.}$$

In the case of neutrinoless double-electron capture, different particles can be emitted: x rays and Auger electrons from de-excitations in atomic shells and γ quanta and/or conversion electrons from de-excitation of daughter nucleus. We suppose here that only one γ quantum is emitted in the nuclear de-excitation process. It should be stressed that the electron captures from different shells ($2K$, KL, $2L$ and other modes) cannot be energetically resolved by our detector. The fit of the measured spectrum in the energy interval 1800–3200 keV (χ^2/d.f. = 37/41 = 0.90, $S = 7 \pm 10$, lim $S = 23$, $\eta = 0.194$) gives the following limit on the $0\nu 2\varepsilon$ transition of ^{106}Cd to the ground state of ^{106}Pd:

$$T_{1/2}^{0\nu 2\varepsilon}(\text{g.s.} \to \text{g.s.}) \geqslant 1.0 \times 10^{21}\ \text{yr at 90 \% CL.}$$

The limits on double-electron capture in ^{106}Cd to the lowest excited levels of ^{106}Pd were obtained by a fit of the data in different energy intervals (see Table IV).

C. Resonant neutrinoless double-electron capture in ^{106}Cd

A resonant neutrinoless double-electron capture in ^{106}Cd is possible on three excited levels of ^{106}Pd with energies of 2718, 2741, and 2748 keV. The half-life of the ^{106}Cd resonant 2ε process was estimated [86] by using the general formalism of Ref. [87] and by calculating the associated nuclear matrix element in a realistic single-particle space with a microscopic nucleon-nucleon interaction. We have used a higher-random-phase-approximation framework called the multiple-commutator model [88,89]. Using the UCOM short-range correlations [90], the half-life for 0ν double-electron capture in ^{106}Cd to the 2718-keV level of ^{106}Pd (assuming that its spin parity is 0^+) can be written as

$$T_{1/2} = (3.0 - 8.1) \times 10^{22} \times \frac{x^2 + 26.2}{\langle m_\nu \rangle^2}\text{yr}, \qquad (1)$$

where $x = \left| Q_{2\beta} - E \right|$ and $\langle m_\nu \rangle$ (the effective Majorana neutrino mass) are in eV units. Here $Q_{2\beta}$ is the difference in atomic mass between ^{106}Cd and ^{106}Pd, and E contains the nuclear excitation energy and the hole energies in the atomic s orbitals. The dependence of the half-life on x is plotted in Fig. 10 for several values of $\langle m_\nu \rangle$. Use of the recently remeasured (by Penning-trap mass spectrometry [32]) value of $Q_{2\beta}$ leads to a value $x = 8390$ eV for the degeneracy parameter and, thus, to the 2ε half-life estimate: $T_{1/2} = (2.1\text{–}5.7) \times 10^{30}$ yr for $\langle m_\nu \rangle = 1$ eV.

We have estimated limits on the resonant $0\nu 2K$ and $0\nu KL$ processes in ^{106}Cd by using the data from our experiment. For instance, the fit of the energy spectrum of the γ and β events measured by the ^{106}CdWO$_4$ detector over 6590 h in the energy region 1280–3000 keV ($\eta = 0.315$) gives 35 ± 34 events for 0ν double-electron captures from two K shells to the excited level at 2718 keV. We should take lim $S = 91$ events, which

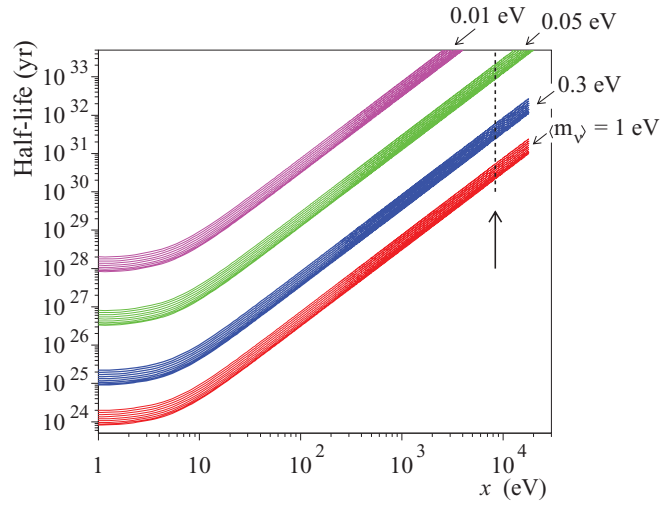

FIG. 10. (Color online) Calculated half-life for resonant $0\nu 2\varepsilon$ capture decay of ^{106}Cd to the excited level 2718 keV of ^{106}Pd as a function of parameter x (see text) for different values of the effective neutrino mass. Dashed line and arrow show the value of x derived from recent measurements of $Q_{2\beta}$ in ^{106}Cd [32].

leads to the following limit on the possible resonant process:

$$T_{1/2}^{0\nu 2K}(\text{g.s.} \to 2718\ \text{keV}) \geqslant 4.3 \times 10^{20}\ \text{yr at 90 \% CL.}$$

For 0ν double-electron capture of K and L_1 electrons to the level 2741 keV, we obtained a slightly stronger restriction ($S = 10 \pm 13$, lim $S = 31$, $\eta = 0.238$):

$$T_{1/2}^{0\nu KL_1}(\text{g.s.} \to 2741\ \text{keV}) \geqslant 9.5 \times 10^{20}\ \text{yr at 90 \% CL.}$$

However, one can expect that the $0\nu KL$ process is strongly suppressed owing to the large spin (4^+) of the level at 2741 keV.

Finally, for 0ν double-electron capture of K and L_3 electrons to the $2, 3^-$ level at 2748 keV, we obtained the following limit ($S = 35 \pm 21$, lim $S = 69$, $\eta = 0.238$):

$$T_{1/2}^{0\nu KL_3}(\text{g.s.} \to 2748\ \text{keV}) \geqslant 4.3 \times 10^{20}\ \text{yr at 90 \% CL.}$$

Despite the fact that the limits are far away from the theoretical predictions, they are higher than the existing limits and are at the level of the best restrictions on resonant processes reported for different isotopes. The limit for 0ν double-electron capture to the level at 2748 keV is obtained for the first time.

All the half-life limits on 2β decay of ^{106}Cd obtained in the present work are summarized in Table IV, where results of the most sensitive previous studies are given for comparison. Although the obtained bounds are well below the existing theoretical predictions [31,34–38], most of the limits are about 1 order of magnitude higher than those previously established. Moreover, some channels of ^{106}Cd double β decay were investigated for the first time. It should be stressed that only two nuclides (^{78}Kr [21] and ^{130}Ba [28]) among six potentially $2\beta^+$ active isotopes [2] were investigated at a comparable level of sensitivity, $T_{1/2} \sim 10^{21}$ yr.

A new phase of the experiment with the ^{106}CdWO$_4$ scintillation detector placed in the ultralow-background GeMulti setup (four HPGe detectors of 225-cm^3 volume each, located at Gran Sasso National Laboratories) is in preparation. We are going

to record pulse profiles and arrival times of the events from the $^{106}CdWO_4$ scintillator in both coincidence and anticoincidence modes. To suppress the background owing to the radioactive contamination of the PMT, the development of a lead tungstate ($PbWO_4$) active light guide from ultrapure archaeological lead [62,91] has been completed. Our preliminary simulations show that such an experiment could investigate the 2ν mode of $\varepsilon\beta^+$ and of $2\beta^+$ decays, and also 2ε transitions of ^{106}Cd to the excited states of ^{106}Pd, at a level of sensitivity near the theoretical predictions: $T_{1/2} \sim 10^{20}$–10^{22} yr [31,34–38].

Moreover, the development of a $^{106}CdWO_4$ crystal scintillator depleted in the ^{113}Cd isotope by a factor of 10^3–10^4 (to reduce the background caused by β decay of $^{113}Cd^m$) is also possible [92]. Such a detector could be able to investigate two-neutrino double-electron capture, which is theoretically the most favorable process of 2β decay of ^{106}Cd.

V. CONCLUSIONS

A low-background experiment using radiopure cadmium tungstate crystal scintillator (215 g) enriched in ^{106}Cd to 66% has been carried out at the underground Gran Sasso National Laboratories of the INFN. The background of the detector below 0.65 MeV is mainly caused by β active $^{113}Cd^m$ ($\approx$116 Bq/kg). We have found surface contamination of the crystal by ^{207}Bi at the level of 3 mBq, which provides a considerable part of the background up to $\approx$2.5 MeV. The activities of U/Th in the scintillator are rather low: $\approx$0.04 mBq/kg of ^{228}Th and $\approx$0.01 mBq/kg of ^{226}Ra. The total α activity of U/Th is at the level of $\approx$2 mBq/kg. The background counting rate of the detector in the vicinity of the ^{106}Cd double β decay energy (2.7–2.9 MeV), after rejection of ^{212}Bi-^{212}Po events, is 0.4 counts/(yr $\times$ keV $\times$ kg).

After 6590 h of data taking, new improved limits on 2β decay of ^{106}Cd were set at the level of 10^{19}–10^{21} yr, in particular, $T_{1/2}^{2\nu\varepsilon\beta^+} \geqslant 2.1 \times 10^{20}$ yr, $T_{1/2}^{2\nu2\beta^+} \geqslant 4.3 \times 10^{20}$ yr, and $T_{1/2}^{0\nu2\varepsilon} \geqslant 1.0 \times 10^{21}$ yr. Resonant $0\nu2\varepsilon$ processes have been restricted to $T_{1/2}^{0\nu2K}$(g.s. $\rightarrow$ 2718 keV) $\geqslant 4.3 \times 10^{20}$ yr; $T_{1/2}^{0\nu KL_1}$(g.s. $\rightarrow$ 2741 keV) $\geqslant 9.5 \times 10^{20}$ yr and $T_{1/2}^{0\nu KL_3}$(g.s. $\rightarrow$ 2748 keV) $\geqslant 4.3 \times 10^{20}$ yr (all confidence limits at 90%). A possible resonant enhancement of $0\nu2\varepsilon$ processes was estimated in the framework of the quasiparticle random phase approximation (QRPA) approach. The half-life of the resonant decay depends on the difference between the value of $Q_{2\beta}$ and the values of the energies of the appropriate excited levels of ^{106}Pd minus the binding energies of two electrons on shells of the daughter atom. The half-life decreases with a decrease in this difference.

The next stage of this experiment is in preparation. We are going to install a low-background scintillation detector with a $^{106}CdWO_4$ crystal into the GeMulti ultralow-background setup with four 225-cm^3 HPGe detectors at Gran Sasso National Laboratories. The sensitivity of the experiment, in particular, to two-neutrino $\varepsilon\beta^+$ decay of ^{106}Cd, is expected to be enhanced thanks to the high-energy resolution of the GeMulti detector and to the improvement of the background conditions in coincidence mode. In addition, we hope to reduce the surface contamination of the scintillator with ^{207}Bi, observed in the present study, by cleaning (removing) the crystal surface. We estimate the sensitivity of the experiment, in particular, to $2\nu\varepsilon\beta^+$ decay of ^{106}Cd, to be at the level of theoretical predictions, $T_{1/2} \sim 10^{20}$–10^{22} yr.

Moreover, a further improvement in sensitivity can be obtained by increasing the enrichment factor of ^{106}Cd and by developing $^{106}CdWO_4$ scintillators with a lower level of radioactive contamination, including depletion of ^{113}Cd. A $^{106}CdWO_4$ scintillation detector with an activity of $^{113}Cd^m$ reduced by a factor of 10^3–10^4 would be able to detect two-neutrino double-electron capture in ^{106}Cd, which is theoretically the most probable process.

ACKNOWLEDGMENTS

The group from the Institute for Nuclear Research (Kyiv, Ukraine) was supported in part by Project Kosmomikrofizyka-2 (Astroparticle Physics) of the National Academy of Sciences of the Ukraine. D. V. Poda and O. G. Polischuk were supported in part by the Project "Double Beta Decay and Neutrino Properties" for young scientists of the National Academy of Sciences of the Ukraine (Reg. No. 0110U004150). The authors would like to express their gratitude to the referee for careful reading of the manuscript and for valuable comments.

[1] F. T. Avignone III, S. R. Elliott, and J. Engel, Rev. Mod. Phys. **80**, 481 (2008); H. V. Klapdor-Kleingrothaus, Int. J. Mod. Phys. E **17**, 505 (2008); H. Ejiri, J. Phys. Soc. Jpn. **74**, 2101 (2005); F. T. Avignone III, G. S. King, and Yu. G. Zdesenko, New J. Phys. **7**, 6 (2005); S. R. Elliot and J. Engel, J. Phys. G **30**, R183 (2004); J. D. Vergados, Phys. Rep. **361**, 1 (2002); S. R. Elliot and P. Vogel, Annu. Rev. Nucl. Part. Sci. **52**, 115 (2002); Yu. G. Zdesenko, Rev. Mod. Phys. **74**, 663 (2002).

[2] V. I. Tretyak and Yu. G. Zdesenko, At. Data Nucl. Data Tables **61**, 43 (1995); **80**, 83 (2002).

[3] A. S. Barabash, Phys. At. Nucl. **73**, 162 (2010).

[4] H. V. Klapdor-Kleingrothaus *et al.*, Eur. Phys. J. A **12**, 147 (2001).

[5] C. E. Aalseth *et al.*, Phys. Rev. D **65**, 092007 (2002).

[6] R. Bernabei *et al.*, Phys. Lett. B **546**, 23 (2002).

[7] F. A. Danevich *et al.*, Phys. Rev. C **68**, 035501 (2003).

[8] E. Andreotti *et al.*, Astropart. Phys. **34**, 822 (2011).

[9] A. S. Barabash, V. B. Brudanin, and NEMO Collaboration, Phys. At. Nucl. **74**, 312 (2011).

[10] H. V. Klapdor-Kleingrothaus and I. V. Krivosheina, Mod. Phys. Lett. A **21**, 1547 (2006).

[11] A. S. Barabash *et al.*, J. Phys. G **34**, 1721 (2007).

[12] H. J. Kim *et al.*, Nucl. Phys. A **793**, 171 (2007).

[13] A. S. Barabash *et al.*, Nucl. Phys. A **807**, 269 (2008).

[14] J. Dawson *et al.*, Nucl. Phys. A **799**, 167 (2008).

[15] P. Belli *et al.*, Phys. Lett. B **658**, 193 (2008).

[16] P. Belli *et al.*, Eur. Phys. J. A **36**, 167 (2008).
[17] A. S. Barabash, P. Hubert, A. Nachab, S. I. Konovalov, and V. Umatov, Phys. Rev. C **80**, 035501 (2009).
[18] P. Belli *et al.*, Eur. Phys. J. A **42**, 171 (2009).
[19] P. Belli *et al.*, Nucl. Phys. A **824**, 101 (2009).
[20] P. Belli *et al.*, Nucl. Phys. A **826**, 256 (2009).
[21] Yu. M. Gavrilyuk *et al.*, Bull. Russ. Acad. Sci. Phys. **75**, 526 (2011).
[22] N. I. Rukhadze *et al.*, Nucl. Phys. A **852**, 197 (2011).
[23] N. I. Rukhadze *et al.*, Bull. Russ. Acad. Sci. Phys. **75**, 879 (2011).
[24] P. Belli *et al.*, J. Phys. G **38**, 015103 (2011).
[25] E. Andreotti *et al.*, Astropart. Phys. **34**, 643 (2011).
[26] A. S. Barabash *et al.*, Phys. Rev. C **83**, 045503 (2011).
[27] P. Belli *et al.*, J. Phys. G **38**, 115107 (2011).
[28] A. P. Meshik, C. M. Hohenberg, O. V. Pravdivtseva, and Y. S. Kapusta, Phys. Rev. C **64**, 035205 (2001).
[29] M. Pujol *et al.*, Geochim. Cosmochim. Acta **73**, 6834 (2009).
[30] R. Cerulli *et al.*, Nucl. Instr. Meth. A **525**, 535 (2004).
[31] M. Hirsch, K. Muto, T. Oda, and H. V. Klapdor-Kleingrothaus, Z. Phys. A **347**, 151 (1994).
[32] M. Goncharov *et al.*, Phys. Rev. C **84**, 028501 (2011).
[33] M. Berglund and M. E. Wieser, Pure Appl. Chem. **83**, 397 (2011).
[34] A. Staudt, K. Muto, and H. V. Klapdor-Kleingrothaus, Phys. Lett. B **268**, 312 (1991).
[35] J. Toivanen and J. Suhonen, Phys. Rev. C **55**, 2314 (1997).
[36] S. Stoica and H. V. Klapdor-Kleingrothaus, Eur. Phys. J. A **17**, 529 (2003).
[37] A. Shukla *et al.*, Eur. Phys. J. A **23**, 235 (2005).
[38] P. Domin *et al.*, Nucl. Phys. A **753**, 337 (2005).
[39] A. S. Barabash *et al.*, Nucl. Phys. A **604**, 115 (1996).
[40] O. A. Rumyantsev and M. H. Urin, Phys. Lett. B **443**, 51 (1998).
[41] O. Civitarese and J. Suhonen, Phys. Rev. C **58**, 1535 (1998).
[42] J. Suhonen and O. Civitarese, Phys. Lett. B **497**, 221 (2001).
[43] R. G. Winter, Phys. Rev. **100**, 142 (1955).
[44] M. B. Voloshin, G. V. Mitselmakher, and R. A. Eramzhyan, JETP Lett. **35**, 656 (1982).
[45] J. Bernabeu, A. de Rujula, and C. Jarlskog, Nucl. Phys. B **223**, 15 (1983).
[46] Z. Sujkowski and S. Wycech, Acta Phys. Pol. B **33**, 471 (2002).
[47] Z. Sujkowski and S. Wycech, Phys. Rev. C **70**, 052501 (2004).
[48] M. I. Krivoruchenko *et al.*, Nucl. Phys. A **859**, 140 (2011).
[49] J. H. Fremlin and M. C. Walters, Proc. Phys. Soc. Lond. A **65**, 911 (1952).
[50] R. G. Winter, Phys. Rev. **99**, 88 (1955).
[51] E. B. Norman and M. A. DeFaccio, Phys. Lett. B **148**, 31 (1984).
[52] D. De Frenne and A. Negret, Nucl. Data Sheets **109**, 943 (2008).
[53] P. Belli *et al.*, Astropart. Phys. **10**, 115 (1999).
[54] Y. Ito *et al.*, Nucl. Instr. Meth. A **386**, 439 (1997).
[55] J. V. Dawson *et al.*, Phys. Rev. C **80**, 025502 (2009).
[56] A. Sh. Georgadze *et al.*, Phys. At. Nucl. **58**, 1093 (1995).
[57] F. A. Danevich *et al.*, Z. Phys. A **355**, 433 (1996).
[58] F. A. Danevich *et al.*, Phys. At. Nucl. **59**, 1 (1996).
[59] F. A. Danevich *et al.*, Phys. Rev. C **67**, 014310 (2003).
[60] P. Belli *et al.*, Phys. Rev. C **76**, 064603 (2007).
[61] P. Belli *et al.*, Nucl. Instr. Meth. A **615**, 301 (2010).
[62] R. S. Boiko *et al.*, Inorg. Mater. **47**, 645 (2011).
[63] P. Belli *et al.*, *Proceedings, International Conference NPAE-2010, 7–12 June 2010, Kyiv, Ukraine* (2011), p. 428; AIP Conf. Proc. **1304**, 354 (2010).
[64] N. I. Rukhadze *et al.*, Phys. At. Nucl. **69**, 2117 (2006).
[65] F. A. Danevich *et al.*, Phys. Lett. B **344**, 72 (1995).
[66] F. A. Danevich *et al.*, Nucl. Phys. A **694**, 375 (2001).
[67] R. B. Firestone *et al.*, *Table of Isotopes*, 8th ed. (John Wiley, New York, 1996) CD update, 1998.
[68] T. Fazzini *et al.*, Nucl. Instr. Meth. A **410**, 213 (1998).
[69] E. Gatti and F. De Martini, *Nuclear Electronics 2, IAEA, Vienna* (1962), p. 265.
[70] L. Bardelli *et al.*, Nucl. Instr. Meth. A **569**, 743 (2006).
[71] P. Belli *et al.*, Nucl. Phys. A **789**, 15 (2007).
[72] G. Bellini *et al.*, Eur. Phys. J. C **19**, 43 (2001).
[73] A. S. Barabash *et al.*, JINST **6**, P08011 (2011).
[74] W. R. Nelson *et al.*, SLAC Report 265, Stanford University (1985).
[75] S. Agostinelli *et al.*, Nucl. Instr. Meth. A **506**, 250 (2003); J. Allison *et al.*, IEEE Trans. Nucl. Sci. **53**, 270 (2006).
[76] O. A. Ponkratenko *et al.*, Phys. At. Nucl. **63**, 1282 (2000); V. I. Tretyak (to be published).
[77] R. Bernabei *et al.*, Nuovo Cimento A **112**, 545 (1999).
[78] M. Günther *et al.*, Phys. Rev. D **55**, 54 (1997).
[79] P. Belli *et al.*, Nucl. Instr. Meth. A **626–627**, 31 (2011).
[80] A. Balysh *et al.*, Prib. Tekh. Eksp. **1**, 118 (1993) (in Russian).
[81] P. de Marcillac *et al.*, Nature **422**, 876 (2003).
[82] N. Coron *et al.*, *Proceedings, Workshop Radiopure Scintillators for EURECA (RPScint'2008), 9-10 September 2008, Kyiv, Ukraine* (Institute for Nuclear Research, Kyiv, Ukraine, 2009), p. 12; arXiv:0903.1539 [nucl-ex].
[83] D. N. Grigoriev *et al.*, Nucl. Instr. Meth. A **623**, 999 (2010).
[84] M. Gunther *et al.*, Phys. Rev. D **55**, 54 (1997).
[85] G. J. Feldman and R. D. Cousins, Phys. Rev. D **57**, 3873 (1998).
[86] J. Suhonen, Phys. Lett. B **701**, 490 (2011).
[87] J. Suhonen and O. Civitarese, Phys. Rep. **300**, 123 (1998).
[88] J. Suhonen, Nucl. Phys. A **563**, 205 (1993).
[89] O. Civitarese and J. Suhonen, Nucl. Phys. A **575**, 251 (1994).
[90] M. Kortelainen *et al.*, Phys. Lett. B **647**, 128 (2007).
[91] F. A. Danevich *et al.*, Nucl. Instr. Methods A **603**, 328 (2009).
[92] A. V. Tikhomirov (private communication).